Green Chemistry

Accepted Manuscript

ROYAL SOCIETY OF CHEMISTRY

www.rsc.org/greenchem

Green Chemistry

ARTICLE

Application of Quaternary Cu_2ZnSnS_4 Quantum Dot-Sensitized Solar Cells Based on Hydrolysis Approach

Bing Bai, Dongxing Kou,* Wenhui Zhou, Zhengji Zhou and Sixin Wu*

www.rsc.org/

The band-tunable quaternary alloy have more excellent photoelectric properties and stability than their binary or ternary components, but their application as sensitizer in quantum dot-sensitized solar cells (QDSSCs) has seldom been reported. The key feature of this problem is that the high fairly small-sized quaternary quantum dots (QDs) require the use of 1-dodecanethiol (DDT) to suppress the growth of QDs, which can not be displaced by bifunctional molecular linker. Herein, we developed a novel synthesis and functionalization strategy for presynthesized Cu_2ZnSnS_4 (CZTS) QDs by utilizing mercapto-acetic acid octyl ester as capping ligand. Unlike the commonly used ligand exchange approach, the long alkyl chains are removed via hydrolysis procedure at pH>7. Benefitting from the broad absorption spectral range, well loading ability and the improvement of electron transport process after ligand hydrolysis, the constructed "green" CZTS QDSSCs finally achieved an impressive conversion efficiency of 3.29% with high short-circuit current of 17.48 $mA \cdot cm^{-2}$ without further modification. This efficiency is the first reported value for CZTS QDSSCs so far, which is comparable to most efficiency for single species sensitizer around 3%, and demonstrates that it is possible to obtain comparable or even better photovoltaic performance than the toxic cadmium or rare indium QDs.

Introduction

Quantum dot sensitized solar cells (QDSSCs) have attracted increasing attention because of their low production cost, size tunable band gap, and high molar extinction coefficient.[1-4] The theoretical efficiency of QDSSCs is as high as 44% in view of multiple exciton generation originating from impact ionization effect.[5] Initially, single binary QD sensitizers such as CdS, CdSe, PbS and PbSe are investigated in QDSSCs,[6] but most of the recorded power conversion efficiency (PCE) values for liquid junction QDSSCs are typically below 7%,[7] remarkably lower than the theoretical efficiency, partially because of the limitation of the light harvesting range of QD sensitizers, the low electron injection efficiency due to the unsatisfied conduction band edge relative to the metal oxide electron conductor (mainly TiO_2), and unsatisfactory surface coverage of QDs on mesoporous oxide film electrodes.[8]

Searching for suitable panchromatic QD sensitizers to expand the light harvesting range without hindering the subsequent electron extraction and ultimately obtaining a high PCE in the resulting cells is a great challenge.[8] Ternary or quaternary alloyed QDs are promising alternative materials to binary QDs due to their optoelectronic properties can be tuned by controlling the composition without changing the particle size,[9, 10] and their band gap has the possibility to be narrower than their binary constituents due to an "optical bowing" effect.[8] Recently, Zhong et al. use high photovoltaic quality core/shell $CuInS_2$ (CIS)/ZnS QDs as sensitizer and achieve a highest efficiency of 7.04%,[11] but this chalcogenide still contains rare indium element.[12]

In comparison, the earth-abundant multicomponent alloy Cu_2ZnSnS_4 (CZTS) and $Cu_2ZnSnSe_4$ (CZTSe) are more alternative materials, because of their comparable photoelectric properties as CIS, such as suitable band gap (1.0-1.8 eV), high absorption coefficient (up to 10^5 cm^{-1}) and good photostability.[13-15] The Cd-, Pb-free CZTS QDs can

The Key Laboratory for Special Functional Materials of MOE, Henan University, Kaifeng, 475004, P. R. China
**E-mail: koudongxing@henu.edu.cn and wusixin@henu.edu.cn*

achieve a higher conduction band than TiO_2 films and a narrower band gap by tuning the Cu:(Zn+Sn) or S/Se ratio without changing the particle size,[9, 10] which will be benefit to the surface coverage of QDs, the light harvesting and the subsequent electron injection.[16] Despite an independently certified 12.6% PCE is recorded in CZTSSe thin-film solar cell,[17] which is even higher than the CIS thin-film solar cell, the application of CZTS QDs in QDSSCs has never been reported. Generally, the main route for immobilization of presynthesized QDs to the TiO_2 electrodes is achieved by the functionalization of QDs, where the weak binded oleylamine or oleic acid is replaced via ligand exchange by bifunctional linker molecules (Figure 1a).[18] However, the high fairly small-sized quaternary CZTS QDs require the use of 1-dodecanethiol (DDT) to shield the surface of the QDs and suppress the growth of QDs into large size by forming strong metal-S bonding.[19] This capping ligand makes the QDs difficult to immobilize on TiO_2 electrode since DDT can not be completely displaced by thioglycolic acid (TGA, a typical bifunctional molecular linker containing a terminal carboxylate group binding to TiO_2 and a thiol group binding to the QDs[20]) during the phase transfer procedure due to the strong coordination capacity of the terminal thiol group.[11, 21] Besides, the long alkyl chains would also act as an insulating layer, impeding the efficient charge transport in TiO_2 electrode and the dissociation of photogenerated excitons.[22] A DDT-free synthesis and immobilization strategy must be developed for the application of CZTS QDs in QDSSCs.

Herein, we developed a novel synthesis and functionalization strategy by utilizing mercapto-acetic acid octyl ester ($HSCH_2COO(CH_2)_7CH_3$) as capping ligand to synthesize CZTS QDs. The key feature of this strategy is to take advantage of the thiol group in bonding with QDs and functionalize the QDs by bifunctional molecular linker. Unlike the commonly used ligand exchange approach, the long alkyl chains are removed via hydrolysis procedure at pH>7 (Figure 1b). Finally, the constructed "green" CZTS QDSSCs achieved an impressive conversion efficiency of 3.29% with high short-circuit current of 17.48 $mA{\cdot}cm^{-2}$ without further modification. This offers a novel functionalization strategy of oil-soluble QDs and opens a new field for the applying of quaternary CZTS QDs in Cd-, Pb- and In-free QDSSCs, which would boost a more powerful efficiency in the future work.

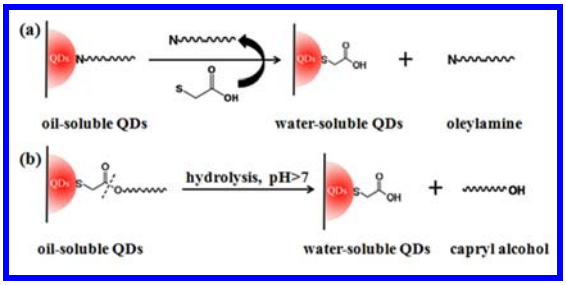

Figure 1 (a) The traditional ligand exchange approach. (b) The hydrolysis strategy of capping ligand.

Experimental

Chemicals

Copper(II) acetylacetonate ($Cu(acac)_2$, 98.5%), Zinc 2,4 pentanedionate monohydrate ($Zn(acac)_2{\cdot}H_2O$), Tin(IV) chloride bis(2,4-pentanedionate) ($Sn(acac)_2Cl_2$, 95%) and thioglycolic acid (TGA, 97%) were purchased from Alfa Aesar. Oleylamine (80-90%) was purchased from Aldrich. Mercapto-acetic acid octyl ester (95.0%) was purchased from TCI. All the chemical reagents were used as received.

Synthesis of CZTS QDs

The oil-soluble CZTS QDs were prepared by one-pot method.[23] Typically, 0.5 mmol $Cu(acac)_2$, 0.25 mmol $Zn(acac)_2{\cdot}H_2O$, 0.25 mmol $Sn(acac)_2Cl_2$, 2.5 ml mercapto-acetic acid octyl ester and 8 ml oleylamine were loaded into a flask. The resulting mixture solution was kept at 80 ^oC under vacuum for 30 min. Subsequently, the solution was heated to 220 ^oC under argon flow and stayed for 45 min. After the flask rapidly cooled down to room temperature, the purified CZTS QDs were obtained by precipitation and centrifugation procedure with the use of ethanol.

Hydrolysis of Capping Ligand

The water-soluble CZTS QDs were obtained by the hydrolysis of capping ligand. Generally, 400 µl TGA was dissolved in 5 ml ethanol. 4 ml CZTS QDs chloroform solution and 2 ml ammonia water were added into the TGA-ethanol solution. Then 2 ml deionized water was added into the mixture after stirred for 1 h at 35 ^oC. The under layer, chloroform, was collected directly and 4 ml ethanol was added and kept stirring for 1 h. After centrifugation, the precipitate was dispersed in 1 ml deionized water for use in the next step. The supernatant was also collected, where the oleylamine and

mercapto-acetic acid octyl ester can be obtained by the distillation of ethanol and reused in the synthesis of CZTS QDs.

Sensitization of TiO_2 Films and Fabrication of Solar Cells

TiO_2 mesoporous electrodes were prepared according to the previous literature [24] and the whole thickness was around 15 μm including a 5 μm light-scattering layer. The photoelectrodes were immersed into QDs deionized water solution for 12 h and then rinsed with water and ethanol sequentially. After deposition, the CZTS QDs-sensitized TiO_2 electrodes were successively dipped into 0.1 M $Zn(NO_3)_2$ solution and 0.1 M Na_2S solution for 3 times to prepare the ZnS passivation layer.

The cells were constructed by sandwiching the photoanodes and the Cu_2S-coated counter electrodes using a 60 μm thermal adhesive film (Surlyn, Dupont). The Cu_2S counter electrodes were prepared by immersing brass foil in 37% HCl solution at 75 °C for 30 min and subsequently washed with water, then followed by sulfidation in the prepared polysulfide solution. The polysulfide electrolyte solution, consisting of 2.0 M Na_2S, 2.0 M S, and 0.2 M KCl in 5 ml deionized water solution, was injected by vacuum backfilling followed with sealing process using a Surlyn film and a cover glass. The active area of the mask covered solar cells was 0.25 cm^2.

Characterization

Transition electron microscopy (TEM) images were obtained by using JSM-2010 instrument. The morphology was characterized by scanning electronic microscope (SEM) equipped with an Energy Dispersive X-Ray Spectroscopy (EDX, Nano SEM 45050/EDX). The crystal structure of CZTS QDs samples was taken on a powder X-ray diffraction (XRD, Bruker D8 Advance, Cu Kα radiation, λ = 1.5406 nm). The Raman spectra of CZTS QDs were collected from a LABRAM-1B confocal laser micro-Raman spectrometer with the wavelength of 632.8 nm. FTIR spectra were performed with a Nicolet 360 FTIR instrument using KBr pellets in the range of 4000-400 cm^{-1}. UV-visible transmission spectra were achieved by using PE-Lambda35. *J-V* characteristics of QDSSCs were derived with a Keithley 2420 digital source meter (Keithley, USA) under a 450W xenon lamp (Oriel Sol3A Solar Simulator 94043, Newport Stratford Inc., USA). The light power density was calibrated against a Si solar cell (Hamamatsu S1133) to accurately simulate the light to 100 mW/cm^2. Electrochemical impedance spectroscopy (EIS) measurements were investigated with a FRA equipped PGSTAT-30 from Autolab (AUT302N, Metrohm, Switzerland). The frequency scan was from 0.1 Hz to 1 MHz.

Results and discussion

The size, shape, surface functionalization, band gap alignment and optoelectronic properties of preprepared QDs can be easily tailored and well controlled via the well-developed organometallic high-temperature synthetic method[23]. We developed a DDT-free CZTS QDs synthesis approach by utilizing mercapto-acetic acid octyl ester as capping ligand. The Cu/Zn/Sn/S ratios of CZTS QDs obtained at different reaction times are listed in Table S1. As the reaction time prolonged, the atomic percentage of Cu reduces from 56.32 to 26.15 before 12 min, while the atomic percentages of Zn, Sn and S gradually increase with the increase of reaction time. The atomic ratios of Cu, Zn, Sn and S are found to be 2.24/1.12/1.22/4 at 12 min, which is close to the 2/1/1/4 stoichiometric ratio, indicating the formation of CZTS QDs. As the reaction time continually increased, the Cu/Zn/Sn/S radios keep constant and the crystallinity of CZTS QDs gradually enhanced, as seen in Figure S1. As discussed above, the formation process of CZTS QDs can be divided into three steps. Firstly, cooper ion is complexed with mercapto-acetic acid octyl ester to form copper-mercapto-acetic acid octyl ester thiolates, which would thermal decompose into Cu_2S at certain temperature. Secondly, zinc and tin gradually enter into the structure of Cu_2S in the crystal growth stage and assist shape transformation to intermediate shaped QDs. Finally, conversion is complete and pure CZTS QDs are obtained.[19,23] The transmission electron microscopy (TEM) images of CZTS QDs are shown in Figure 2. It can be seen that fairly monodisperse CZTS QDs with the average size of about 3.5 nm is obtained.

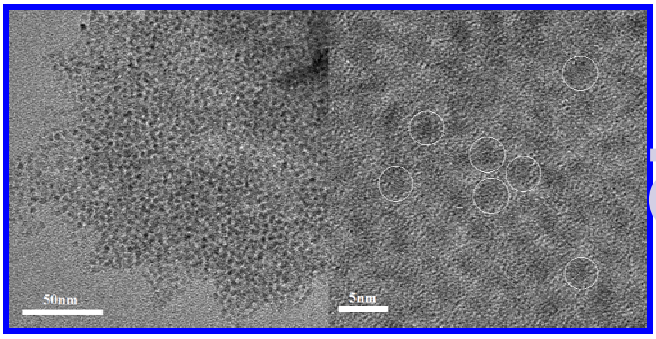

Figure 2 TEM images of as-synthesized CZTS QDs. (a) scale bar, 50 nm. (b) scale bar, 5 nm.

In order to efficiently immobilize QDs onto mesoporous TiO_2 film with high loading, the as-prepared oil-soluble QDs should first

convert into water-soluble QDs via ligand exchange, during which the native long hydrocarbon chain around the QDs surface are replaced by the bifunctional hydrophilic TGA ligand. Since the strong coordination thiol group used here can not be replaced, we prepared the TGA-capped QDs and remove the long hydrocarbon chain via hydrolysis procedure at pH>7. Figure 3 shows the FTIR spectra of preprepared CZTS QDs before and after ligand hydrolysis. After ligand hydrolysis, the stretching vibration of -C=O (1730 cm^{-1}) in mercapto-acetic acid octyl ester disappears and the presence of the symmetric (1379 cm^{-1}) and asymmetric (1558 cm^{-1}) stretching vibration are assign to the COO^- group in ionized TGA.[25, 26] Meanwhile, the characteristic absorption peak of -NH_2 (1643 cm^{-1}) in oleylamine also disappears, indicating the removement of oleylamine by TGA.[27] The capping TGA on the water-soluble QDs should come from both ligand hydrolysis and the replacement of oleylamine.

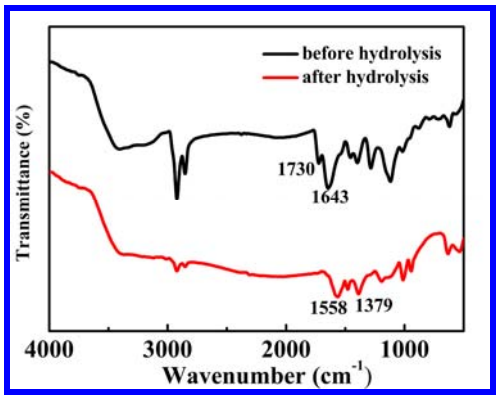

Figure 3 FTIR spectra of CZTS QDs before and after ligand hydrolysis

Figure 4a shows XRD patterns of the oil-soluble and water-soluble CZTS QDs. The diffraction peaks appear at 28.5°, 47.3° and 56.1°, consistent with the (112), (220) and (312), matching well with kesterite-phase CZTS (JCPDS 26-0575).[28] However, it should be noted that only XRD patterns can't determine the phase purity of quaternary CZTS QDs accurately because much binary and ternary chalcogenides have similar crystal structures.[13,29] Raman spectroscopy is further employed for phase analysis of the CZTS QDs, as shown in Figure 4b. The Raman peaks of oil-soluble and water-soluble CZTS QDs both locate at about 333 cm^{-1}, which are in good agreement with the data presented before.[30] Both XRD and Raman patterns present no other characteristic peaks of impurities, such as $Cu_{2-x}S$ and ZnS,[29] indicating that the pure kesterite-phase CZTS QDs are obtained and ligand hydrolysis don't change the structure of CZTS QDs.

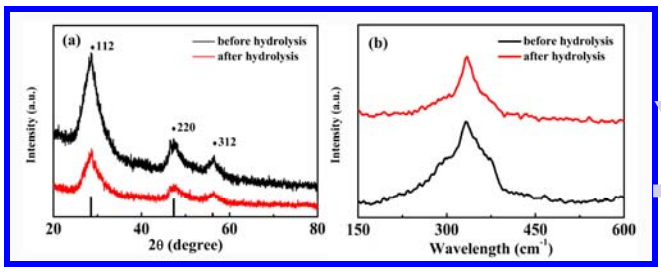

Figure 4 (a) XRD patterns of oil-soluble and water-soluble CZTS QDs. (b) Raman spectra of oil-soluble and water-soluble QDs.

Figure 5 illustrates the UV-vis absorption spectra of oil-soluble and water-soluble QDs dispersions. It can be seen that the absorption spectroscopy of water-soluble QDs is similar to that of oil-soluble QDs. The light harvesting range of both sensitized films covers the whole visible spectrum and extends to NIR region with wavelength as far as 900 nm. This broad absorption spectral range will enhance the light harvesting efficiency and pave the way for high photocurrent in the resulting QDSSCs.

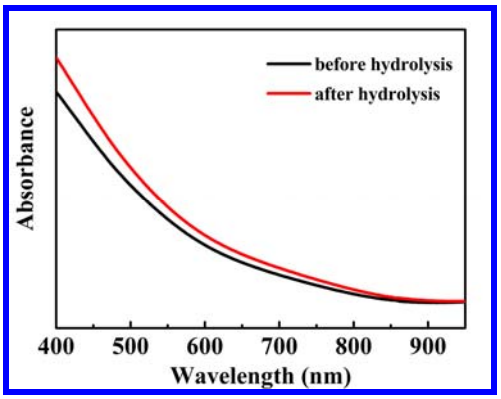

Figure 5 UV-vis absorption spectra of oil-soluble and water-soluble QDs.

Even though the organometallic synthetic method can support high-quality CZTS QDs and contribute a broad absorption spectral range, it is still a great challenge to assemble preprepared QDs onto TiO_2 electrodes with high surface coverage. The cross-sectional EDX images in Figure 6 give direct evidence to estimate the QDs loading ability and their distribution over TiO_2 films. With the aim of imaging the QD sensitizer on the TiO_2 surface directly, we deposited the QDs on TiO_2 films without a scattering layer. The elemental mappings of Ti, Cu, Zn, Sn and S demonstrate an uniform coverage of QDs throughout the 10.3 μm films and their atomic percentages are found to be 16.32, 3.26, 1.60, 1.89 and 6.07%, which is close to the 2/1/1/4 stoichiometric ratio of Cu/Zn/Sn/S.[31] The high QD loading in our case can be ascribed to the synthesis of small-sized

CZTS QDs, penetrating into the porous network of TiO_2 films, and the access of highly stable TGA-capped QDs aqueous solution for long time dispersion.

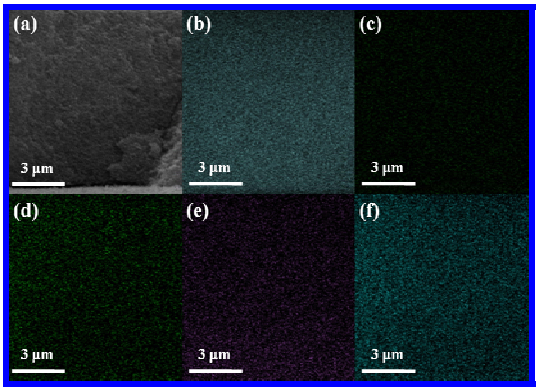

Figure 6 (a) Cross-section of SEM image of a TiO_2 films, element distribution maps of (b) Ti, (c) Cu, (d) Zn, (e) Sn and (f) S. Scale bar, 3 μm.

To further reveal the interfacial behavior of injected electrons in the QDSSCs after ligand hydrolysis, electrochemistry impedance spectroscopy (EIS) analysis was performed under a forward bias of -0.30 V, as seen in Figure 7. The radius of the semicircle in the middle-frequency area are corresponding to the 45° line diffusion resistance related to electron transport in TiO_2 films and the charge-transfer resistance related to recombination of electrons at the TiO_2/electrolyte interface.[32] A more extended diffusion line can be found for the QDSSCs before ligand hydrolysis and the diffusion line nearly disappeared after hydrolysis, indicating that the electron transport process is improved by the removement of long hydrocarbon chains. This will further support a higher photocurrent in the QDSSCs after ligand hydrolysis.

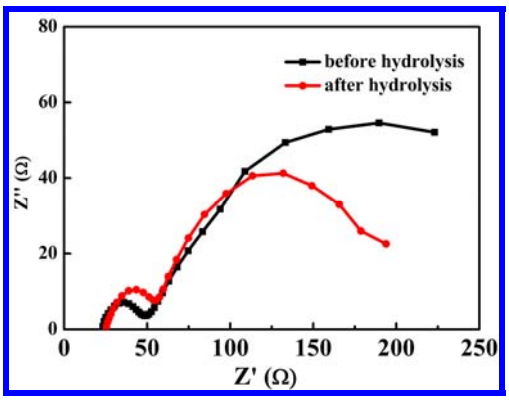

Figure 7 EIS spectra of CZTS QDSSCs before and after ligand hydrolysis.

Incident photon to electron conversion efficiency (IPCE) of QDSSCs before and after ligand hydrolysis are plotted in Figure 8a. It is found that the photocurrent response starts at near 900 nm for both cells and the overall photocurrent response closely matches the corresponding absorption spectra of QDs as shown in Figure 5. It has been established that IPCE can be calculated from the equation: IPCE=LHE×ϕ_{inj}×η_c,[11] where LHE, ϕ_{inj} and η_c is the light absorption efficiency, electron injection efficiency and charge collection efficiency, respectively. Zhu[22] has proposed that the ϕ_{inj} of water-soluble QDs is higher than the oil-soluble one. In our experiment, the η_c can be also improved due to the remarkable decrease of diffusion resistance after ligand hydrolysis. As a result, both the improvement of electron injection efficiency and charge collection efficiency contribute a remarkable higher IPCE than that of QDSSCs before ligand hydrolysis. The *J-V* characteristics of QDSSCs before and after ligand hydrolysis are presented in Figure 8b. An impressive enhancement in three parameters can be found for TGA-capped CZTS QDSSCs due to the improvement of light harvesting and electron transport as discussed before. It is meaningful to note that a high short-circuit current of 17.48 mA·cm^{-2} and a conversion efficiency of 3.29% was achieved without further modification. To our knowledge, this PCE is the first reported value for CZTS QDSSCs so far, and is comparable to most efficiency for single species sensitizer around 3%.[22,33] However, the efficiency is still limited by low open-circuit voltage and fill factor due to the intrinsic property of CZTS QDs. Future strategies, such as the better band level matching with TiO_2 films, the enhancement of crystallization to decrease the trap states and the access of surface passivation barrier to depress recombination, need to be further developed.

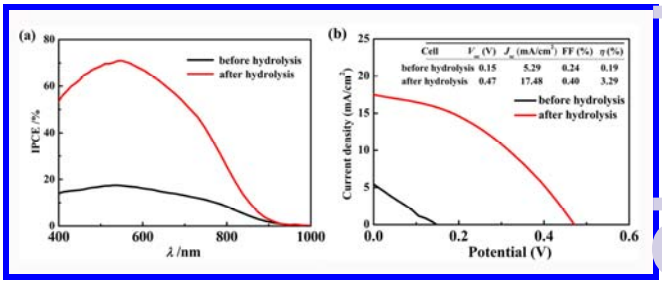

Figure 8 (a) Incident Photon to Current Efficiency. (b) *J-V* characteristics of CZTS QDSSCs under AM 1.5 with typical organic ligand capped CZTS QDs sensitizer and TGA-capped CZTS QDs sensitizer.

Conclusions

In conclusion, we opened a new field for the applying of band-tunable quaternary CZTS QDs into QDSSCs by functionalizing oil-soluble CZTS QDs via a novel hydrolysis strategy. The constructed "green" CZTS QDSSCs finally achieved an impressive conversion efficiency of 3.29% with high short-circuit current of 17.48 $mA \cdot cm^{-2}$ without further modification, mainly attributed to the broad absorption spectral range, well loading ability and the improvement of electron transport process after ligand hydrolysis. Further strategies will be developed to boost a more powerful efficiency in the future work, such as type-I and type-II band level alignments, the enhancement of crystallization and the surface passivation.

Acknowledgements

This project is supported by the National Natural Science Foundation of China (21203053, 21271064 and 61306016), the Joint Talent Cultivation Funds of NSFC-HN (U1204214), the Program for Changjiang Scholars and Innovative Research Team in University (PCS IRT1126) of Henan University.

References

1 B. Oregan and M. Grätzel, *Nature,* 1991, **353**, 737.
2 P. V. Kamat, *J. Phys. Chem. Lett.* 2013**, 4**, 908.
3 D. V. Freitas, J. M. M. Dias, S. G. B. Passos, G. C. S. de Souza, E. T. Neto and M. Navarro, *Green Chem.* 2014, **16**, 3247.
4 K. Kim, I. Kim, Y. Oh, D. Lee, K. Woo, S. Jeong and J. Moon, *Green Chem.* 2014, **16**, 4323.
5 I. P. Liu, C.-W. Chang, H. Teng and Y.-L Lee, *ACS Appl. Mater. Interfaces* 2014, **6**, 19378.
6 Z. S. Yang, C. Y. Chen, P. Roy and H. T. Chang, *Chem. Commun.* 2011, **47**, 9561.
7 S. Jiao, Q.; Shen, I. Mora-Seró, J. Wang, Z. Pan, K. Zhao, Y. Kuga, X. Zhong and J. Bisquert, *ACS Nano* 2015, **9**, 908.
8 Z. Pan, K. Zhao, J. Wang, H. Zhang, Y. Feng and X Zhong, *ACS Nano* 2013, **7**, 5215.
9 P. C. Dai, X. N. Shen, Z. J. Lin, Z. Y. Feng, H. Xu and J. H. Zhan, *Chem. Commun.* 2010, **46**, 5749.
10 S. C.;Riha, B. A. Parkinson and A. L. Prieto, *J. Am. Chem. Soc.* 2011, **133**, 15272.
11 Z. X. Pan, I. Mora-Sero, Q. Shen, H. Zhang, Y. Li, K. Zhao, J. Wang, X. H. Zhong and J.Bisquert, *J. Am. Chem. Soc.* 2014, **136**, 9203.
12 A. V. Moholkar, S. S. Shinde, A. R. Babar, K. U. Sim, Y. b. Kwon, K. Y. Rajpure, P. S. Patil, C. H. Bhosale and J. H. Kim, *Sol. Energy* 2011, **85**, 1354.
13 S. C. Riha, B. A. Parkinson and A. L. Prieto, *J. Am. Chem. Soc.* 2009, **131**, 12054.
14 Q. Tian, L. Huang, W. Zhao, Y. Yang, G. Wang and D. Pan, *Green Chem.* 2015, **17**, 1269.
15 J. Zhong, Z. Xia, C. Zhang, B. Li, X. Liu, Y. B. Cheng and J. Tang, *Chem. Mater.* 2014, **26**, 3573.
16 H. McDaniel, N. Fuke, J. M. Pietryga and V. I. Klimov, *J. Phys. Chem. Lett.* 2013, **4**, 355.
17 W. Wang, M. T. Winkler, O. Gunawan, T. Gokmen, T. K. Todorov, Y. Zhu and D. B. Mitzi, *Adv. Energy Mater.* 2014, **4**, 1301465.
18 R. S. Selinsky, Q. Ding, M. S. Faber, J. C. Wright and S. Jin *Chem. Soc. Rev.* 2013, **42**, 2963.
19 Y. Liu, D. Yao, L. Shen, H. Zhang, X. D. Zhang and B. Yang, *J. Am. Chem. Soc.* 2012, **134**, 7207.
20 D. Lawless, S. Kapoor and D. Meisel, *J. Phys. Chem.* 1995, **99**, 10329.
21 C. C. Chang, J. K. Chen, C. P. Chen, C. H. Yang and J. Y. Chang, *ACS Appl. Mater. Interfaces* 2013, **5**, 11296.
22 F. Liu, J. Zhu, J. F. Wei, Y. Li, L. H. Hu, Y. Huang, O. Takuya, Q. Shen, T. Toyoda, B. Zhang, J. X. Yao and S. Y. Dai, *J. Phys. Chem. C.* 2014, **118**, 214.
23 M. Li, W. H. Zhou, J. Guo, Y. L. Zhou, Z. L. Hou, J. Jiao, Z. J. Zhou, Z. L. Du and S. X. Wu, *J. Phys. Chem. C.* 2012, **116**, 26507.
24 L. H. Hu, S. Y. Dai, J. Weng, S. F. Xiao, Y. F. Sui, Y. Huang, S. H. Chen, F. T. Kong, X. Pan, L. Y. Liang and K. J. Wang, *J. Phys. Chem. B.* 2007, **111**, 358.
25 C. Wang, X. Gao, Q. Ma and X. G. Su, *J. Mater. Chem.* 2009, **19**, 7016.
26 M. S. High, P. C. Painter and M. M. Coleman, *Macromolecules* 1992, **25**, 797.
27 J. Luo, L. Y. Wang, D. Mott, P. N. Njoki, N. Kariuki, C. J. Zhong and T. He, *J. Mater. Chem.* 2006, **16**, 1665.
28 B. S. Tosun, B. D. Chernomordik, A. A. Gunawan, B. Williams K. A. Mkhoyan, L. F. Francis and E. S. Aydil, *Chem. Commun.* 2013, **49**, 3549.
29 Y. Kim, K. Woo, I. Kim, Y. S. Cho, S. Jeong and J. Moon, *Nanoscale* 2013, **5**, 10183.
30 A. Singh, H. Geaney, F. Laffir and K. M. Ryan, *J. Am. Chem. Soc.* 2012, **134**, 2910.
31 C. A. Cattley, C. Cheng, S. M. Fairclough, L. M. Droessler, N. P Young, J. H. Warner, J. M. Smith, H. E. Assender and A. A. R.

Watt, *Chem. Commun.* 2013, **49**, 3745.

32 F. Fabregat-Santiago, J. Bisquert, G. Garcia-Belmonte, G. Boschloo and A. Hagfeldt, *Sol .Energy Mater. Sol. Cells* 2005, **87**, 117.

33 D. H. Jara, S. J. Yoon, K. G. Stamplecoskie and P. V. Kamat, *Chem. Mater.* 2014, **26**, 7221.